

Geometry dependent dephasing in small metallic wires

D. Natelson, R.L. Willett, K.W. West, L.N. Pfeiffer
Bell Laboratories, Lucent Technologies, Murray Hill, NJ 07974
(November 1, 2018)

Temperature dependent weak localization is measured in metallic nanowires in a previously unexplored size regime down to width $w = 5$ nm. The dephasing time, τ_ϕ , shows a low temperature T dependence close to quasi-1D theoretical expectations ($\tau_\phi \sim T^{-2/3}$) in the narrowest wires, but exhibits a relative saturation as $T \rightarrow 0$ for wide samples of the same material, as observed previously. As only sample geometry is varied to exhibit both suppression and divergence of τ_ϕ , this finding provides a new constraint on models of dephasing phenomena.

Quantum mechanical decoherence in metals is an outstanding problem in condensed matter physics. Magnetotransport measurements in a number of quasi-1D and quasi-2D systems at the smallest accessible size scales have shown an unexpected saturation in the weak localization magnetoresistance (WLMR) at low temperatures, interpreted as a saturation of the coherence time τ_ϕ as $T \rightarrow 0$ [1,2]. These observations run counter to theoretical expectations [3,4,5], since the inelastic processes that cause decoherence are expected to freeze out as $T \rightarrow 0$, implying that τ_ϕ should diverge in this limit. In diffusive, metallic, quasi-1D systems the expected form of the divergence is $T^{-2/3}$ due to electron-electron scattering [3]. Subsequent experiments have shown reasonable agreement with theory in degenerately doped semiconducting wires [6], and a strong material dependence of the saturation in evaporated metals [7]. This experimental situation has prompted a number of theoretical [8,9,10,11,12,13,14,15] responses. An intrinsic saturation of τ_ϕ to a finite value as $T \rightarrow 0$ would have profound implications for the ground state of metals and might indicate a fundamental limitation in controlling quantum coherence in conductors. The physical mechanism underlying the saturation of the WLMR remains a subject of controversy. Establishing a controlled experimental parameter influencing this saturation would provide a starting point for modeling possible dephasing mechanisms.

The WLMR results from pairs of time-reversed loop trajectories that contribute coherently to the conductance [3,4,5]. In a system with a diffusion constant D , the relevant scale for coherence is $L_\phi \equiv \sqrt{D\tau_\phi}$, and the scale for thermal smearing is $L_T \equiv \sqrt{\hbar D/k_B T}$. The quasi-1D regime occurs in samples of width w and thickness t when $L_\phi, L_T > w, t$, while quasi-2D behavior is expected when $t < L_\phi, L_T < w$. Threading magnetic flux through a typical trajectory suppresses the contribution of such loops, resulting in a MR whose size and field-scale reflect the sample geometry and L_ϕ . Analysis of the WLMR provides an estimate of τ_ϕ .

In this Letter, we present transport studies of AuPd nanowires with a range of widths showing that extremely narrow wires in an unexplored quasi-1D regime

($w = 5$ nm) have a WLMR that agrees with the theoretical functional T dependence from 4.2 K to below 0.1 K; increasing sample width in this same material suppresses the temperature dependence, with quasi-2D wires ($w = 1.2 \mu\text{m}$) having WLMR consistent with the saturation seen in previous quasi-2D studies of this metal [16,2]. Data at intermediate widths indicate an evolution from one behavior to the other. This is the first observation that the phase coherence as a function of temperature of a metal can be tuned from suppressed to diverging by varying an externally controlled parameter, in this case sample geometry. Access to this regime is achieved by using metal wires narrower than 50 nm.

Table I summarizes sample dimensions and properties. The smallest width samples (A-F) were fabricated using a nonlithographic “edge” technique [18] (see Fig. 1), while samples G-K were defined using electron beam lithography (EBL) and liftoff processing on undoped (100) GaAs substrates. The edge technique uses selective chemistry to produce precise nanoscale relief on the cleaved (0 $\bar{1}1$) face of an undoped MBE-grown GaAs/AlGaAs wafer. Metal deposition and directional etching are then used to produce nanowires with widths set by MBE growth precision. The wire material for each sample consisted of a 1 nm Ti adhesion layer followed by 7.5 nm of Au_{0.6}Pd_{0.4} deposited by electron beam evaporation at a base pressure of 2×10^{-7} Torr. For all samples a lead frame was then defined using EBL, and made by e-beam evaporation of 2.5 nm of Ti and 90 nm of Au with subsequent liftoff.

Sheet resistances of codeposited films were measured at 4.2 K. Typical resistivity of deposited films is found to be $\sim 24 \mu\Omega\text{-cm}$, consistent with other investigators’ evaporated AuPd films [16]. Free electron values for the density of states ν and Fermi velocity v_F for pure Au [21] were combined with the Einstein relation to estimate the diffusion constant D and the elastic mean free path $\ell \sim 2 - 3$ nm from measured film resistivities.

Contact resistances between the leads and wires were on the order of a few Ohms, while typical lead resistances were 100-200 Ω . At the lead-wire contact point, the leads were $\sim 0.5 \mu\text{m}$ wide. The interlead spacing L is the distance between “inner” edges of voltage leads (see

Fig. 1). These lengths were considerably greater than ℓ and L_ϕ (as analyzed below), suppressing “non-local” four-terminal resistance effects [17].

Samples were mounted on a dilution refrigerator, with “bath” temperature measured using a calibrated Ge resistance thermometer. Resistances were measured using lock-in techniques at a frequencies ≤ 17 Hz. For samples A-E, two- and four-terminal measurements were employed with similar results, while the remaining samples were only examined with a four-terminal bridge method. Measurement currents were maintained at levels low enough to avoid Joule heating (0.05 nA for samples A-E, 0.5 nA for sample F, <5 nA for samples G-K). Two checks on this were performed: R continued to vary down to the lowest temperatures, and there both $R(H=0)$ and $R(H)$ were unchanged when the measuring current was reduced by a factor of two. Magnetic fields as large as 8 T were applied transverse to the direction of current in the wires.

Figure 2 shows magnetoresistance data for various sample widths and summarizes our key finding: varying sample width alters the MR temperature dependence. The positive sign of the MR is consistent with previous observations [16] that AuPd is a strong spin-orbit scattering system. The data are symmetric in field, so only positive field direction sweeps are shown. The data for the 5 nm-wide sample (sample A) are shown in Fig. 2a; MR data for H in the other transverse direction were similar. The shape of the MR curves is consistent with a quasi-1D dimensionality ($L_\phi > d, t$). The MR is temperature-dependent over the entire range, increasing from $\sim 2.5\%$ at 4.2 K to roughly 15% at 100 mK, and the field scale at which $\Delta R/R$ saturates moves to smaller fields as T is decreased. At temperatures less than 0.5 K aperiodic variations of $\Delta R/R$ with H are visible. Such sample-specific fluctuations varied from cooldown to cooldown, and are universal conductance fluctuations as a function of external field.

Compare these curves with the analogous MR data for a quasi-2D 1.2 μm -wide wire (sample K) shown in Fig. 2d. The size and field scale of the MR effect are consistent with the dimensionality and resistance per square of the sample. However, the MR is only weakly dependent on temperature over the entire range, varying from 0.04% to 0.055%, in contrast to the narrow wire data. Fig. 2c shows MR traces for an array of 0.12 μm -wide wires, expected to be of intermediate dimensionality (almost quasi-2D at 4.2 K, almost quasi-1D at 0.1 K). For this intermediate size, the temperature dependence of the overall MR effect is slightly larger in size than the results for the widest wires. Fig. 2b shows MR data for 20 nm-wide wires, expected to be in the quasi-1D limit over the entire temperature range; the temperature dependence of MR data with H in the other transverse direction was similar. The MR temperature dependence is more pronounced than the 0.12 μm case, but not as large as in the

5 nm wires. The raw data in Fig. 2 show that the temperature dependence of the MR in a single material increases substantially as the width of the wires is reduced, independent of the analysis of the MR as a measure of electronic coherence in these samples.

We use the theory of weak localization to extract a characteristic dephasing time, τ_ϕ , from the MR data. Analytic MR predictions exist for samples of definite dimensionality, and an internally consistent analysis requires, *e.g.*, the extracted $\sqrt{D\tau_\phi} > d, t$ if a quasi-1D formula was used. The relevant MR predicted [3,23] for the quasi-1D case is:

$$\frac{\Delta R}{R} = \frac{1}{\pi\sqrt{2}} \frac{e^2 R}{\hbar L} \sqrt{D\tau_N} \times f\left(\frac{2\tau_N}{\tau_{\phi 0}}\right), \quad (1)$$

with $f(x) \equiv \text{Ai}(x)/\text{Ai}'(x)$, where $\text{Ai}(x)$ is the Airy function. Here τ_N is the time associated with coherence loss due to small angle Nyquist electron-electron scattering. The rate $\tau_{\phi 0}^{-1}$ is the sum of large energy ($\sim k_B T$) scattering processes at $H=0$ and the magnetic contribution, $\tau_H^{-1} = DW^2/12L_H^4$, with $L_H = \sqrt{\hbar/2eH}$. Here W is the sample dimension transverse to the applied magnetic field. To minimize the number of fitting parameters, we fix W at 5 nm for samples A-E and 20 nm for sample F; we use D as inferred from the codeposited film; and we set the time $\tau_{\phi 0}(H=0)$ to some long value (100 ns). Using measured values of R and L at each temperature, the only remaining variational parameter is τ_N . We limit the fitting with Eq. (1) to the field regime $L_H > W$ and avoid large conductance fluctuations. The theoretical prediction for the quasi-1D Nyquist scattering time is given by:

$$\tau_{N,\text{th}} = \left(\frac{\hbar^2 L}{e^2 \sqrt{2D} k_B T R} \right)^{2/3}. \quad (2)$$

For the quasi-2D case (samples H-K), the appropriate magnetoresistance prediction is [19,16]:

$$\frac{\Delta R}{R} = \frac{R_\square e^2}{4\pi^2 \hbar} \left[\psi\left(\frac{1}{2} + \frac{L_H^2}{2D\tau_\phi}\right) - \ln\left(\frac{L_H^2}{2D\tau_\phi}\right) \right], \quad (3)$$

where $\psi(x)$ is the digamma function. To fit the data we use the measured resistance per square R_\square , D as inferred from the resistivity, and allow τ_ϕ in Eq. (3) to vary.

Figure 3 shows the results of fitting the MR data for representative samples, 5 nm-wide samples A and B, 20 nm-wide sample F, and wider samples J and K. The other samples show similar behavior. The scatter in the fit parameter τ_N is dominated by variation in the MR data due to universal conductance fluctuations [17,22,18]. For samples A-E, $\tau_N(T)$ was fit to the form KT^p , yielding $p = -0.59 \pm 0.05$, consistent with the predicted T dependence of Eq. (2). The prefactor K found in samples A-E is approximately a factor of four smaller than that predicted by Eq. (2), consistent with previous investigations [23,20,7].

In contrast with this consistency between the experimental results and theory, consider the $\tau_\phi(T)$ parameters extracted from wide samples J and K using Eq. (3). The weak temperature dependence of τ_ϕ in these wider samples is as seen in previous studies of quasi-2D samples of AuPd [16]. Note that the quasi-2D prediction for Nyquist dephasing is an even steeper temperature dependence than the quasi-1d case, $\tau_{\phi,2D} \sim T^{-1}$ [3], and for $R_\square \approx 32\Omega$, $\tau_{\phi,2D} \sim 6 \times 10^{-9}$ s at 1 K. These experimental findings support an empirical picture in this material of τ_ϕ evolving from a form consistent with e-e interactions to one not understood as sample width is increased toward 2D. Attempts to analyze the suppressed MR data using a sum of two different dephasing rates are complicated by the small size of the MR effects in the widest samples.

Proposed mechanisms for the anomalous saturation of τ_ϕ as $T \rightarrow 0$ must be considered in light of the size dependence reported here. The cause of the saturation in the widest wires remains unknown at this time, and may well involve an additional phase-breaking mechanism with a weak T dependence over the interval examined. Any explanation based on the intrinsic properties of the material must reconcile the observed variation of the saturation with sample size, and with metal, since τ_ϕ in Ag wires has been seen to not saturate down to 40 mK, while saturation was seen at ~ 700 mK in Cu wires with similar parameters [7]. Careful examination of these metals over size ranges is warranted.

Our observations also constrain possible extrinsic sources of dephasing. Since overall sample resistances for the widest and narrowest wires were of the same order (~ 10 k Ω), it is unlikely that external RF noise [6,9] can account for the difference in WLMR behaviors.

One plausible explanation for the geometry-dependence of the MR is competition between Nyquist scattering and an unknown dephasing mechanism. Both processes presumably exist in all the samples, but for fixed disorder smaller sample dimensions enhance the Nyquist process (see Eq. (2)) by increasing R/L . It is possible that in sufficiently narrow wires, the Nyquist dephasing rate τ_N^{-1} becomes more rapid than the competing process, while in wide wires the other process could dominate as the Nyquist scattering rate is reduced. Alternately, the unknown dephasing mechanism may be suppressed as sample size is reduced below some crucial lengthscale. Detailed studies of the size dependence in this and other materials and extensions to lower temperatures, while significant experimental challenges, may help distinguish these possibilities.

We have examined magnetotransport as $T \rightarrow 0$ in AuPd nanowires down to wire widths substantially below 10 nm, demonstrating that a single material system can exhibit either saturating or diverging magnetoresistance behavior depending on sample geometry. When analyzed within the framework of WL theory, this translates into a difference in inferred dephasing behaviors. The narrowest wires seem qualitatively consistent with the predictions for Nyquist dephasing in quasi-1D systems, while wide wires exhibit a saturation of τ_ϕ similar to that seen in previous investigations. With the evidence that geometry can tune MR behavior between saturating and nonsaturating regimes, we have a new tool for examining the properties of τ_ϕ .

We thank B.L. Altshuler, K. Baldwin, R. dePicciotto, E.M.Q. Jariwala, P. Mohanty, P.M. Platzman, S. Simon, and C.M. Varma for valuable discussions.

Sample	w [nm]	t [nm]	L [μm]	D [m^2/s]	R/L or R_\square [@ 4.2 K]
A	5	7.5	1.5	1.2×10^{-3}	19.2 k $\Omega/\mu\text{m}$
B	5	7.5	1.5	1.2×10^{-3}	17.0 k $\Omega/\mu\text{m}$
C	5	7.5	1.5	1.5×10^{-3}	14.9 k $\Omega/\mu\text{m}$
D	5	7.5	1.5	1.5×10^{-3}	14.1 k $\Omega/\mu\text{m}$
E	5	7.5	0.75	1.5×10^{-3}	14.8 k $\Omega/\mu\text{m}$
F	20	7.5	1.5	1.5×10^{-3}	3.6 k $\Omega/\mu\text{m}$
G	120	7.5	6.6	1.5×10^{-3}	265 $\Omega/\mu\text{m}$
H	1100	7.5	380	1.5×10^{-3}	31.5 Ω/\square
I	1100	7.5	380	1.5×10^{-3}	31.5 Ω/\square
J	1250	7.5	380	1.5×10^{-3}	32.3 Ω/\square
K	1250	7.5	380	1.5×10^{-3}	32.3 Ω/\square

TABLE I. Samples used in magnetotransport measurements. To minimize “magnetofingerprint” effects, Sample F is an average of two 1.5 μm segments, while Sample G is an array of 19 wires in parallel, for which single-wire parameters are listed.

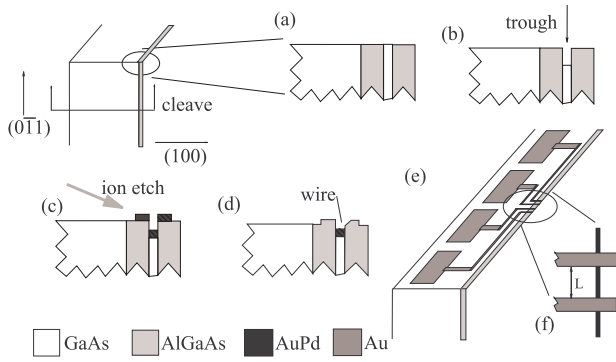


FIG. 1. The edge wire fabrication process. (a) MBE-grown substrate is cleaved; (b) EBL is used to expose the thin GaAs layer, which is selectively etched to produce a trough; (c) Wire material is deposited, the resist is lifted off, and a directional ion etch removes excess material; (d) a nanowire is left in the trough, ready for further EBL to define leads; (e); Wire length L is defined by spacing of voltage leads, as shown in (f).

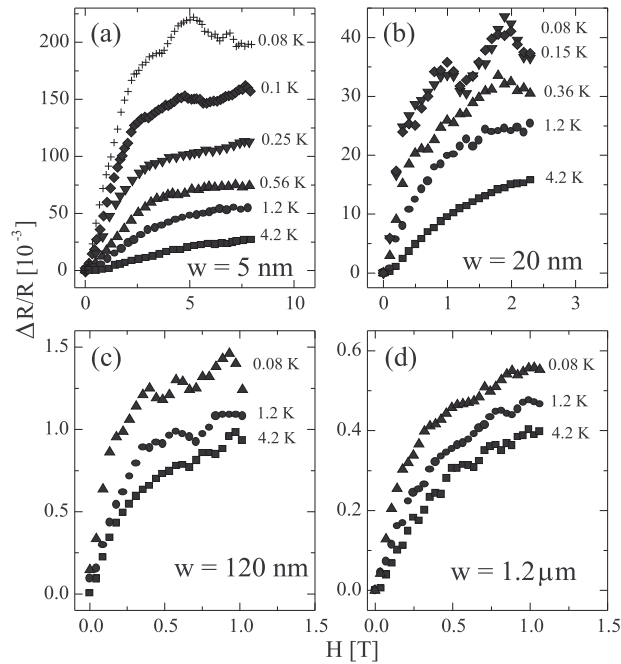


FIG. 2. Perpendicular magnetoresistance curves for representative samples, plotted as $(R(T, H) - R(T, 0))/R(T, 0)$ vs. H . The WLMR is symmetric about zero field. (a) Sample A, H along (100), $w = 5$ nm, quasi-1D; (b) Sample F, H along (011), $w = 20$ nm, quasi-1D; (c) Sample G, array of 19 wires in parallel, H along (100), $w = 0.12$ μm , intermediate dimensionality; (d) Sample K, H along (100), $w = 1.2$ μm , quasi-2D.

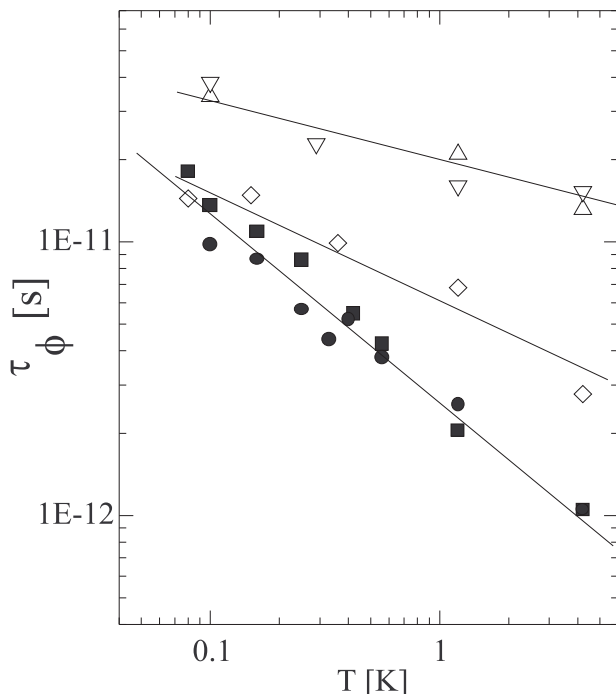


FIG. 3. Coherence times as a function of temperature, extracted using Eqs. (1) and (3) for samples (A = ■, B=●, F=◇) and (J=▽, K=△), respectively. Data for (J,K) have been vertically offset (multiplied by 2.5) for clarity; lines are a guide to the eye, and top to bottom correspond to power laws of $T^{-0.22}$, $T^{-0.40}$, and $T^{-0.67}$.

- [1] P. Mohanty, E.M.Q. Jariwala, and R.A. Webb, Phys. Rev. Lett. **78**, 3366 (1997).
- [2] R.A. Webb, P. Mohanty, and E.M.Q. Jariwala, Fortschr. Phys. **46**, 779 (1998).
- [3] B.L. Altshuler, A.G. Aronov, D.E. Khmel'nitskii, J. Phys. C **15**, 7367 (1982).
- [4] P. Lee and T.V. Ramakrishnan, Rev. Mod. Phys. **57**, 287 (1985).
- [5] Y. Imry, *Introduction to Mesoscopic Physics*, (Oxford University Press, 1997).
- [6] Yu. B. Khavlin, M.E. Gershenson, A.L. Bogdanov, Phys. Rev. Lett. **81**, 1066 (1998).
- [7] A.B. Gougam, F. Pierre, H. Pothier, D. Esteve, and N.O. Birge, J. Low Temp. Phys. **118**, 447 (2000).
- [8] P. Mohanty and R.A. Webb, Phys. Rev. B **55**, 13452 (1997).
- [9] B.L. Altshuler, M.E. Gershenson, and I.L. Aleiner, Physica E **3**, 58 (1998); I.L. Aleiner, B.L. Altshuler, and M.E. Gershenson, Wave Rand. Med. **9**, 201 (1999).
- [10] D.S. Golubev and A.D. Zaikin, Phys. Rev. Lett. **81**, 1074 (1998); D.S. Golubev and A.D. Zaikin, Physica B **255**, 164 (1998); D.S. Golubev and A.D. Zaikin, Phys. Rev. B **59**, 9195 (1999); A.D. Zaikin and D.S. Golubev, Physica B **280**, 453 (2000).
- [11] K. Houshangpour and K. Maschke, Phys. Rev. B **59**, 4615 (1999).
- [12] Y. Imry, H. Yukuyama, P. Schwab, Europhys. Lett. **47**, 608 (1999);
- [13] A. Zawadowski, J. von Delft, and D. Ralph, Phys. Rev. Lett. **83**, 2632 (1999).
- [14] R. Krishnan and V. Srivastava, Phys. Rev. B **59**, R12747 (2000).
- [15] X.R. Wang, G. Xiong, and S.D. Wang, Phys. Rev. B **61**, R5090 (2000).
- [16] J.J. Lin and N. Giordano, Phys. Rev. B **35**, 1071 (1987) and references.
- [17] S. Washburn and R.A. Webb, Rep. Prog. Phys. **55**, 1311 (1992).
- [18] D. Natelson, R.L. Willett, L.N. Pfeiffer, and K.W. West, Sol. State Comm., in press.
- [19] S. Hikami, A.I. Larkin, and Y. Nagaoka, Prog. Theor. Phys. **63**, 707 (1980).
- [20] M.E. Gershenson, Ann. der Physik **8**, 559 (1999).
- [21] N.W. Ashcroft and N.D. Mermin, *Solid State Physics* (Holt, Rinehart, and Winston, New York, 1976).
- [22] S. Feng, *Mesoscopic Phenomena in Solids*, ed. B.L. Al'tshuler, P.A. Lee, R.A. Webb (Elsevier, 1991) 107, N. Giordano, *ibid.*, 131.
- [23] P.M. Echternach, M.E. Gershenson, H.M. Bozler, A.L. Bogdanov, B. Nilsson, Phys. Rev. B **48**, 11516 (1993).